as fetuses and infants (Sinder, 1994; Bibel and Barde, 2000). If the effect of BDNF as an accelerator, not as a neurotrophin, on the methylmercury-induced cell death in vitro is also detected in the brain, the indispensability of BDNF for normal development of nerve tissue might determine the higher sensitivity to methylmercury in developing animals. The second characteristic is that neurons highly sensitive to methylmercury toxicity, such as cerebellar granular cells and granular cells of the cerebral cortex, are in particular areas of the central nervous system (Tsubaki and Irukayama, 1977; Weiss et al., 2002), which means that the difference in sensitivity to methylmercury occurs between neurons even in the same brain. In the present study, BDNF promoted methylmercury-induced death of TrkB-expressing cells, suggesting that neurons which express TrkB will be more sensitive to methylmercury than those which do not. Thus, the difference in methylmercury sensitivity between neurons in the brain may be determined by whether or not individual neurons express TrkB. And in fact, the second to fifth layers of the cerebral cortex of humans show higher levels of TrkB mRNA, while the second and following layers show a higher expression of BDNF mRNA (Webster et al., 2006), which is in partial agreement with the layers of the human cerebral cortex that are degenerated by methylmercury exposure, particularly the second and third layers (Takeuchi et al., 1977). The BDNF-induced acceleration of methylmercury-induced cell death is a good model to clarify the mechanisms of this BDNF effect. Further investigation using this model may help to identify the mechanisms and characteristics of methylmercury toxicity.

4. Experimental Procedures

4.1. Cell cultures and treatment

Primary cultures of cerebellar granule neurons were prepared from Wistar rats

(Jcl:Wistar; Clea Co., Tokyo, Japan) within 24 h after birth, as described previously (Sakaue et al., 2005). Briefly, cerebella were removed from the pups and incubated with trypsin for 13 min at room temperature were minced by mild triturating with a Pasteur pipette. Cerebellar granule cells were seeded in Eagle's minimal essential medium (Gibco BRL, Grand Island, NY) containing 1 mg/ml BSA, 10 μg/ml bovine insulin, 0.1 nM thyroxin, 0.1 μg/mg human transferrin, 1 μg/ml aprotinin, 30 nM Na_2SeO_3, 0.25% glucose, 100 units /mL penicillin, and 135 μg/mL streptomycin on poly-L-lysine-coated dishes and cultured for 2 days. Rat neuroblastoma B35 cells were purchased from the American Type Culture Collection (ATCC, Manassas, VA). The B35 cells were cultured in growth medium, Dulbecco's modified Eagle's medium supplemented with 10% fetal calf serum (HyClone, South Logan, UT), 100 units /mL penicillin, and 135 μg/mL streptomycin. The medium was changed every second day. These cell culture supplements were purchased from Sigma-Aldrich (St. Louis, MO).

The cells were pre-incubated for 24 h and treated with methylmercuric chloride (Tokyo Kasei Kogyo, Co., Ltd., Tokyo, Japan) at the concentrations indicated in the figures with or without recombinant human BDNF (Peprotech, London, UK), recombinant human neurotorophin-4 (NT-4; Sigma-Aldrich), or mouse nerve growth factor (NGFβ; Sigma-Aldrich). These neurotrophins were added to the medium 30 min before the methylmercury treatment. In addition, a BDNF-neutralizing antibody (Sigma-Aldrich) and a MAPK inhibitor, U0126 (Calbiochem, Darmstadt, Germany), were used to investigate whether the BDNF effect involves the binding of BDNF to its receptor and activation of the MAP signaling cascade. The numbers of viable cells of the primary culture and the B35 cell line were estimated by crystal violet staining, as described previously (Sakaue et al., 2005). All experiments were carried out in

accordance with the Kitasato University Guidelines for Animal Care and Experimentation.

4.2. Cloning of the stable transformant of B35 cells expressing TrkB

Using two primers, rTrkB1FEcoRI (5'-GAATTCCTGGCGTATAGGAC-3') and rTrkB1RNotI (5'-GCGGCCGCACTGTCAGAGCGAA-3'), designated on the sequences of rat TrkB from GenBank (Accession No. NM_012731), rat TrkB cDNA was amplified with rat brain cDNA as a template. An approximately 2.8-kb cDNA fragment of TrkB was cloned into the EcoRI/NotI site of pcDNA3.1 (Invitrogen, Carlsbad, CA) for construction of the expression plasmid and then sequenced.

B35 cells were transfected with the TrkB expression construct using Lipofectamin (Invitrogen, Carlsbad, CA) according to the manufacturer's instructions. Stable transformants were selected in growth medium containing 0.8 mg/ml geneticin (G418; Invitrogen). G418-resistant cells were cloned, and the TrkB mRNA expression was checked in each clone using RT-PCR. To confirm the function of the expressed TrkB protein in the transformant, phosphorylation of two factors of signal transduction in the region downstream of TrkB, ERK and MEK, in the selected clone in mock or TrkB transformants after BDNF treatment was detected using Western blot analysis, which was performed as described in our previous report (Sakaue et al., 2005). Briefly, after BDNF treatment at 50 ng/ml, B35 cells were washed three times with PBS (pH 7.4) and harvested in Lamini's buffer (3% SDS, 62.5 mM Tris base, pH 6.8). The protein concentration in cell lysates was determined by a BCA assay (Bio-Rad, Hercules, CA). SDS-polyacrylamide gel electrophoresis (PAGE) was performed with 50 μg of lysate protein. For Western blotting, proteins were transferred to a PVDF membrane (GE Healthcare, Buckinghamshire, UK) at 100 V for 2 h. To determine the phosphorylation

state, the membrane was washed in 0.05% Tween-20 PBS (T-PBS) and incubated in a blocking buffer, 1% bovine serum albumin T-PBS, for 1 h at room temperature. Then, the first antibody, i.e., rabbit anti-phospho-ERK (pERK) 1/2 antibody, anti-ERK1/2 antibody, anti phospho-MEK antibody or anti-MEK antibody, was reacted with the membrane for 12 h at 4°C, followed by reaction with horseradish peroxidase-conjugated secondary antibody (1:1000; Sigma) for 1 h at 4°C. These antibodies were purchased from Cell Signaling Technology, Inc. (Danvers, MA). Enhanced chemiluminescence by Chemilumi one (Nacali Tesque, Kyoto, Japan) was determined by exposure to an X-ray film (GE Healthcare).

4.3. RT-PCR

Total RNAs of rat cerebellar neuronal culture and whole cerebella were extracted and reverse-transcribed in a reaction solution containing SuperScript™ II reverse transcriptase and Oligo(dT)$_{12-18}$Primer (Invitrogen) for producing cDNA, as described previously (Sakaue et al., 2002). The cDNAs were stocked at -20°C before use. PCRs for TrkA, TrkB, and TrkC were carried out in 50 µl of PCR mixture containing 1.25 units of ExTaq™ polymerase (Takara Biochemicals, Otsu, Japan), 1 x ExTaq™ buffer, 0.2 mM dNTP mixture, 100 pM of each primer, and 2 µl of the cDNA. The PCR conditions for all genes were as follows: an initial denaturation step at 95°C for 3 min, followed by 40 cycles of denaturation at 95°C for 30 sec, annealing at 60°C for 30 sec, and extension at 72°C for 45 sec, with a final extension step at 72°C for 3 min. The primer sequences of the neurotrophin receptors reported by Nemoto et al. (2000) were referenced in the present study.

Acknowledgements

This study was supported by a grant (no. 20780221, to MS) from the Ministry of

Education, Culture, Sports, Science, and Technology of Japan, by a project grant (Young Scientist Research Training Award, 2008) from the Azabu University Research Services Division (to MS), and by a grant from The Morinaga Foundation for Health & Nutrition (to MS).

References

Aschner, M., Du, Y.L., Kimelberg, H.K., 1993. Methylmercury-induced alterations in excitatory amino acid transport in rat primary astrocyte cultures. Brain Res. 602, 181-186.

Bakir, F., Damluji, S.F., Amin-Zaki, L., Murtadha, M., Khalidi, A., al-Rawi, N.Y., Tikriti, S., Dahahir, H.I., Clarkson, T.W., Smith, J.C., Doherty, R.A., 1973. Methylmercury poisoning in Iraq. Science 191, 230-241.

Bibel, M., Barde, Y.A., 2000. Neurotrophins: key regulators of cell fate and cell shape in the vertebrate nervous system. Genes Dev. 14, 2919-2937.

Castoldi, A.F., Barni, S., Turin, I., Gandini, C., Manzo, L., 2000. Early acute necrosis, delayed apoptosis and cytoskeletal breakdown in cultured cerebellar granule neurons exposed to methylmercury. J. Neurosci. Res. 60, 775-787.

Dare, E., Götz, M.E., Zhivotovsky, B., Manzo, L., Ceccatelli, S., 2000. Antioxidants J811 and 17beta-estradiol protect cerebellar granule cells from methylmercury-induced apoptotic cell death. J. Neurosci. Res. 62, 557-565.

Harada, Y., 1968. Congenital (or fetal) Minamata disease. In Minamata Disease, Study group of Miminamata Disease, ed. Kumamoto University, Kumamoto, pp. 93-118.

Marsh, D.O., Myers, G.J., Clarkson, T.W., Amin-Zaki, L., Tikriti, L., Majeed, M.A., 1980. Fetal methylmercury poisoning: Clinical and toxicological data on 29 cases. Ann. Neurol. 7, 348-353.

Marty, M.S., Atchison, W.D., 1997. Pathways mediating Ca^{2+} entry in rat cerebellar granule cells following in vitro exposure to methylmercury. Toxicol. Appl. Pharmacol. 147, 319-330.

Miyamoto, K., Nakanishi, H., Moriguchi, S., Fukuyama, N., Eto, K., Wakamiya, J., Murao, K., Arimura, K., Osame, M., 2001. Involvement of enhanced sensitivity of N-methyl-D-aspartate receptors in vulnerability of developing cortical neurons to methylmercury neurotoxicity. Brain. Res. 901, 252-258.

Nemoto, K., Miyata, S., Nemoto, F., Yasumoto, T., Murai, U., Kageyama, H., Degawa, M., 2000. Gene expression of neurotrophins and their receptors in lead nitrate-induced rat liver hyperplasia. Biochem. Biophys. Res. Commun. 275, 472-476.

Park, S.T., Lim, K.T., Chung, Y.T., Kim, S.U., 1996. Methylmercury-induced neurotoxicity in cerebral neuron culture is blocked by antioxidants and NMDA receptor antagonists. Neurotoxicol. 17, 37-46.

Reichardt, L.F., 2006. Neurotrophin-regulated signaling pathways. Phil. Trans. R. Soc B 361, 1545-1564.

Sakaue, M., Adachi, T., Okazaki, M., Nakamura, H., Mori, N., Hara, S., Sakabe, K., 2006. Effects of sodium selenite on methylmercury-induced cell death and on mercury accumulation in rat cerebellar neurons in primary culture. Bull. Environ. Contam. Toxicol. 77, 779-784.

Sakaue, M., Ishimura, R., Kurosawa, S., Fukuzawa, N.H., Kurohmaru, M., Hayashi, Y., Tohyama, C., Ohsako S., 2002. Administration of estradiol-3-benzoate down-regulates the expression of testicular steroidogenic enzyme genes for testosterone production in the adult rat. J. Vet. Med. Sci. 64, 107-113.

Sakaue, M., Mori, N., Okazaki, M., Ishii, M., Inagaki, Y., Iino, Y., Miyahara, K.,

Yamamoto, M., Kumagai, T., Hara, S., Yamamoto, M., Arishima, K., 2008. Involvement of independent mechanism upon poly(ADP-ribose) polymerase (PARP) activation in methylmercury cytotoxicity in rat cerebellar granule cell culture. J. Neurosci. Res. 86, 3427-3434.

Sakaue, M., Okazaki, M., Hara, S., 2005. Very low levels of methylmercury induce cell death of cultured rat cerebellar neurons via calpain activation. Toxicology 213, 97-106.

Sanchez-Perez, A.M., Llansola, M., Felipo, V., 2006. Modulation of NMDA receptors by AKT kinase. Neurochem. Inter. 49, 351-358.

Sarafian, T., Verity, M.A., 1991. Oxidative mechanisms underlying methylmercury neurotoxicity. Int. J. Dev. Neurosci. 9, 147-153.

Sinder, W.D., 1994. Functions of the neurotrophins during nervous system development: what the knockouts are teaching us. Cell 77, 627-638.

Takeuchi, T., 1968. Pathology of Minamata disease. In Minamata Disease, Study Group of Minamata Disease, ed. Kumamoto University, Kumamoto, pp 141-228.

Takeuchi, T., Eto, K., 1977. Pathology and pathogenesis of Minamata disease. In Minamata Disease: Methylmercury Poisoning in Minamata and Niigata, Japan, Tsubaki, T. and Irukayama, K., eds. Kodansha, Tokyo, pp. 103-141.

Webster, M.J., Herman, M.M., Kleinman, J.E., Weickert, C.S., 2006. BDNF and trkB mRNA expression in the hippocampus and temporal cortex during the human lifespan. Gene Expression Patterns 6, 941-951.

Weiss, B., Clarkson, T.W., Simon., W., 2002. Silent latency periods in methylmercury poisoning and in neurodegenerative disease. Env. Health Perspect. 110 (suppl 5), 851-854.

Xu, F., Plummer, M.R., Len, G.W., Nakazawa, T., Yamamoto, T., Black, I.B., Wu, K., 2006. Brain-derived neurotrophic factor rapidly increases NMDA receptor channel activity through Fyn-mediated phosphorylation. Brain Res. 1121, 22-34.

Figure legends

Fig. 1. BDNF accelerates methylmercury-induced cell death in a primary culture of rat cerebellar granule cells. (A-D) Phase-contrast micrographs of cerebellar granular cells in BDNF-treated culture. The microphotographs show (A) control, (B) methylmercury-treated (30 nM), (C) BDNF-treated (100 ng/ml), and (D) methylmercury and BDNF-treated (30 nM and 100 ng/ml) cells. Bar = 50 μm. Cerebellar granule cell viability was assayed 48 h after treatment with methylmercury (30 nM) and/or with the neurotrophins (E and F) BDNF, (G) NT-4, or (H) NGFβ. (F) Alteration of the BDNF effect at 100 ng/ml on the cell viability over time. Data are expressed as the mean ± S.D. (E, G, H, n = 3; F, n = 4) of the percentage of cell viability compared to the group without methylmercury and BDNF treatments. Statistical analyses were performed using two-way ANOVA with Fisher's PLSD test as a post-hoc test. *, a, b, c, and d denote significant differences between different letters ($p < 0.05$).

Fig. 2. Involvement of TrkB and its signal cascade in the acceleration of methylmercury-induced cell death by BDNF treatment (10 ng/ml). Cell viability was assayed 48 h after methylmercury treatment at 30 nM. (A) Inhibitory effect of the neutralizing antibody against BDNF and (B) inhibitory effect of the MAPK inhibitor, U0126 (30 μM) on the augmentation of cell death by BDNF. (A and B) Data are expressed as the mean ± S.D. (A, n = 4; B, n = 3) of the percentage of cell viability compared to the group without methylmercury and BDNF treatments. Statistical analyses were performed using two-way ANOVA with Fisher's PLSD test as a post-hoc test. a, b, c, d, and e denote significant differences between different letters ($p < 0.05$).

(C) RT-PCR analysis of the mRNA expression of neurotrophin receptors in a primary culture of rat cerebellar granule cells (lane #1 and 2) and cerebrum (lane #3). The cDNAs for the PCR templates were synthesized from total RNA that was independently prepared from the primary cultures of rat cerebellar granule cells or the whole cerebrum of an adult rat.

Fig. 3. TrkB expression is necessary for BDNF to act as an accelerator for methylmercury-induced cell death in the stable transformant of the TrkB expression vector. The cells, mock (A, C, E, G) and TrkB (B, D, F, H) transformants, were incubated and then fixed 40 h after methylmercury treatment. Phase-contrast micrographs show the results in (A, B) control, (C, D) BDNF-treated, (E, F) CH_3HgCl-treated, (G, H) or BDNF plus CH_3HgCl-treated cells. (I) Viability of the stable transformant 40 h after treatment. The concentration of BDNF is 100 ng/ml. Bar = 100 μm. (J) BDNF alters the viability of the TrkB transformant cells in a dose-dependent manner. The TrkB transformant cells were incubated with methylmercury at 0 nM (white bar) or 600 nM (black bar). Data are expressed as the mean ± S.D. (n = 3) of the percentage of cell viability to mock control at (I) or to control treated with 0 nM of methylmercury at (J). Statistical analyses were performed using two-way ANOVA with Fisher's PLSD test as a post-hoc test. a, b, c, d, and e denote significant differences between different letters ($p < 0.05$). (K) Detection of phosphorylated ERK (pERK) and MEK (pMEK) to confirm the function of the expressed TrkB in the mock or TrkB transformants with (+) or without (-) BDNF treatment. Cell lysates were subjected to Western blotting, and the results were confirmed with anti-pERK, anti-ERK, anti-pMEK or anti-MEK antibodies.

Figure

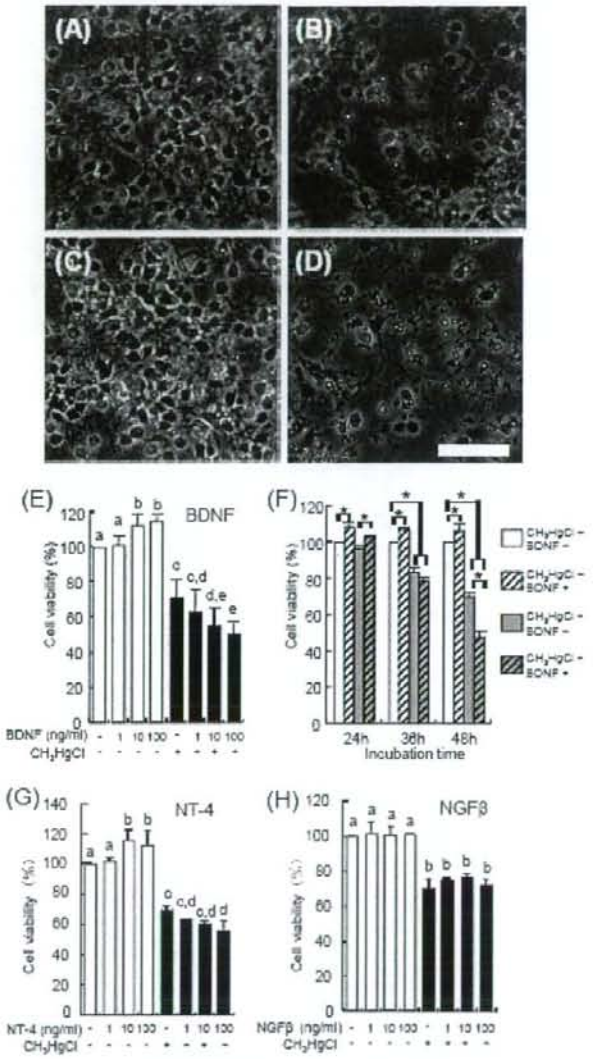

Figure 1

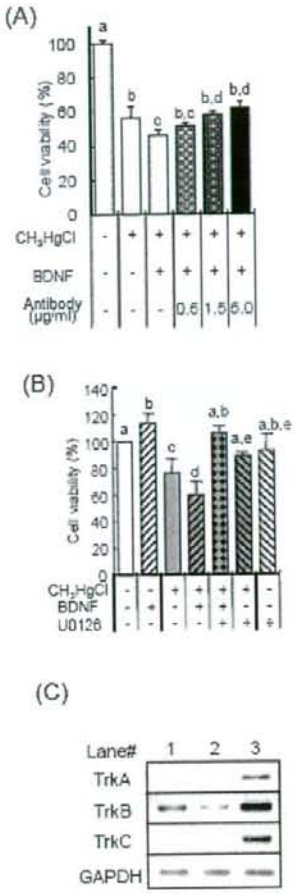

Figure 2

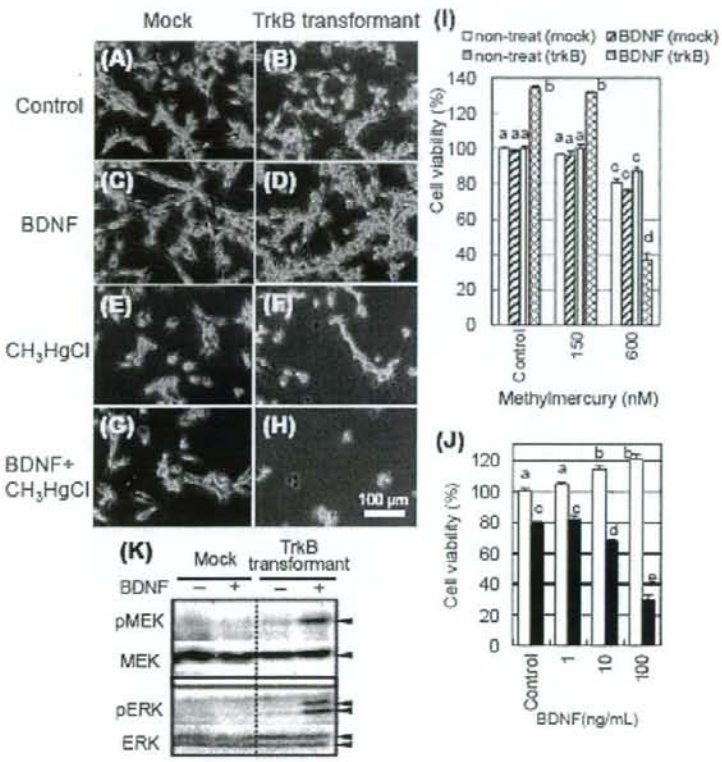
Mock
TrkB transformant
(A)
(B)
Control
(C)
(D)
BDNF
(E)
(F)
CH3HgCl
(G)
(H)
BDNF+
CH3HgCl
100 μm
(I)
non-treat (mock)
BDNF (mock)
non-treat (trkB)
BDNF (trkB)
Cell viability (%)
Control
150
600
Methylmercury (nM)
(J)
Cell viability (%)
Control
1
10
100
BDNF(ng/mL)
(K)
Mock
TrkB transformant
BDNF
pMEK
MEK
pERK
ERK

Figure 3

Microsomal prostaglandin E synthase-1 in both cancer cells and hosts contributes to tumor growth, invasion and metastasis

Daisuke KAMEI[*†], Makoto MURAKAMI[*‡¶], Yuka SASAKI[*], Yoshihito NAKATANI[*], Masataka MAJIMA[§], Yukio ISHIKAWA[#], Toshiharu ISHII[#], Satoshi UEMATSU[⁑], Shizuo AKIRA[⁑], Shuntaro HARA[*1] and Ichiro KUDO[*⁂]

[*]The Department of Health Chemistry, School of Pharmacy, Showa University, 1-5-8 Hatanodai, Shinagawa-ku, Tokyo 142-8555, Japan; [†]the Department of Research and Development for Innovative Medical Needs, School of Pharmacy, Showa University, 1-5-8 Hatanodai, Shinagawa-ku, Tokyo 142-8555, Japan; [‡]the Tokyo Metropolitan Institute of Medical Science, 3-18-22 Bunkyo-ku, Tokyo 113-8613, Japan; [¶]PRESTO, Japan Science and Technology Agency, 4-1-8 Honcho Kawaguchi, Saitama 332-0012, Japan; [§]Department of Pharmacology, School of Medicine, Kitasato University, 1-15-1 Kitasato, Sagamihara, Kanagawa 228-8555, Japan; [#]Department of Pathology, School of Medicine, Toho University, 5-21-16 Omori-Nishi, Ohta-ku, Tokyo 143-8540, Japan; and [⁑]the Department of Host Defense, Research Institute for Microbial Diseases, Osaka University, 3-1 Yamada-oka, Suita, Osaka 565-0871, Japan.

Short title: mPGES-1 and tumorigenesis

[1]To whom correspondence should be addressed. Shuntaro Hara, Ph. D., The Department of Health Chemistry, School of Pharmacy, Showa University, 1-5-8 Hatanodai, Shinagawa-ku, Tokyo 142-8555, Japan. Phone: +81-3-3784-8196. Fax: +81-3-3784-8245. E-mail: haras@pharm.showa-u.ac.jp

Abbreviations used: mPGES-1, microsomal prostaglandin E synthase-1; PG, prostaglandin; COX, cyclooxygenase; LLC, lewis lung carcinoma; KD, knockdown; KO, knockout; NSAIDs, nonsteroidal anti-inflammatory drugs; EPs, PGE receptors; DMEM, Dulbecco's modified Eagle's medium; FCS, fetal calf serum; WT, wild-type; $dmPGE_2$, 16,16-dimethyl PGE_2; TBS, tris-buffered saline; VEGF, vascular endothelial growth factor; PBS, phosphate-buffered saline; EDTA, ethylenediaminetetraacetic acid; ECM, extracellular matrix; MMPs, matrix metalloproteinases.

Synopsis

Microsomal prostaglandin E synthase-1 (mPGES-1) is a stimulus-inducible enzyme that functions downstream of cyclooxygenase (COX)-2 in the prostaglandin E_2 (PGE_2)-biosynthetic pathway. Although COX-2-derived PGE_2 is known to play a role in the development of various tumors, the involvement of mPGES-1 in carcinogenesis has not yet been fully understood. Here, we used Lewis lung carcinoma (LLC) cells with mPGES-1 knockdown or overexpression as well as mPGES-1-deficient mice to examine the roles of cancer cell- and host-associated mPGES-1 in the processes of tumorigenesis *in vitro* and *in vivo*. We found that siRNA silencing of mPGES-1 in LLC cells decreased PGE_2 synthesis markedly, accompanied by reduced cell proliferation, attenuated Matrigel invasiveness and increased extracellular matrix adhesion. Conversely, mPGES-1-overexpressing LLC cells showed increased proliferating and invasive capacities. When implanted subcutaneously into wild-type mice, mPGES-1-silenced cells formed smaller xenograft tumors than did control cells. Furthermore, LLC tumors grafted subcutaneously into mPGES-1 KO mice grew more slowly than did those grafted into littermate wild-type mice, with concomitant decreases in the density of microvascular networks, the expression of proangiogenic vascular endothelial growth factor, and the activity of matrix metalloproteinase-2. Lung metastasis of intravenously injected LLC cells was also significantly less obvious in mPGES-1-null mice than in wild-type mice. Thus, our present approaches provide unequivocal evidence for critical roles of the mPGES-1-dependent PGE_2 biosynthetic pathway in both cancer cells and host microenvironments in tumor growth and metastasis.

Key words: microsomal prostaglandin E synthase-1, prostaglandin E_2, tumorigenesis, knockout mouse, metastasis.

INTRODUCTION

Numerous studies on rodent cancer models and human cancers have shown that nonsteroidal anti-inflammatory drugs (NSAIDs) have antineoplastic properties [1]. A well-known effect of the NSAIDs is their ability to inhibit the enzyme cyclooxygenase (COX) and thereby to suppress prostaglandin (PG) synthesis. PGE_2, the most common PG, is involved in tumor progression by inducing angiogenesis, invasion, and metastasis in several solid tumors [2]. Biosynthesis of PGE_2 from arachidonic acid, which is spatiotemporally supplied from membrane phospholipids by the action of phospholipase A_2, is catalyzed sequentially by COX and PGE synthase (PGES) [3]. COX catalyzes the insertion of molecular oxygen into arachidonic acid to form the unstable intermediate PGG_2, which is rapidly converted to PGH_2 by the peroxidase activity of the same enzyme. Of the two COX isoforms, COX-1 is expressed constitutively in most tissues and is generally responsible for the production of PGs that control normal physiological functions, while COX-2 is inducible in response to mitogens, cytokines, and cellular transformation. High levels of constitutive expression of COX-2 and its product PGE_2 have been detected in various cancer cells and tissues. Moreover, pharmacological, cell biological, and gene targeting studies investigating COX-2 and PGE receptors (EPs) have demonstrated that PGE_2 produced through the COX-2-dependent pathway contributes to the progression of several types of cancer [4, 5].

PGES catalyzes the conversion of PGH_2, produced by COX-1 or COX-2, to PGE_2. Thus far, three PGES enzymes, microsomal PGES (mPGES)-1, mPGES-2, and cytosolic PGES (cPGES), have been identified [6-9]. Among these PGES isozymes, mPGES-1 is induced by proinflammatory stimuli and down-regulated by anti-inflammatory glucocorticoids as in the case of COX-2, and is functionally coupled with COX-2 in marked preference to COX-1 [7, 10, 11]. Induction of mPGES-1 expression and its function have been observed in various diseases and systems in which COX-2-driven PGE_2 has been implicated, such as rheumatoid arthritis, febrile response, reproduction, bone metabolism, cardiovascular function, stroke, and Alzheimer's disease [12, 13]. Furthermore, it has recently been reported that mPGES-1 is constitutively expressed in several cancers, most of which also express COX-2 constitutively [14, 15]. We have reported that the forcible transfection of mPGES-1 in combination with COX-2, but not with COX-1, into HEK293 cells led to cellular transformation with a concomitant and robust increase in PGE_2 [14]. Transgenic mice overexpressing both COX-2 and mPGES-1 developed metaplasia, hyperplasia, and tumorous growth in the glandular stomach with heavy macrophage infiltration [16, 17]. It has also been suggested that the PGE_2 produced through the COX-2-dependent pathway may regulate cancer-host communications that influence tumor progression. Studies using mice null for COX-2 or EPs have revealed that stromal cells around cancer cells express COX-2 and synthesize PGE_2, which, in tumor niches, may act on stromal cells in an autocrine fashion to induce the production of proangiogenic factors and consequent angiogenesis as well as on cancer cells in a paracrine fashion to promote their growth, survival, adhesion and motility [5, 18-20]. Although several studies, including ours, have found by immunohistochemistry that mPGES-1 is expressed in both stromal cells and cancer cells in tumor tissues [14, 21], the contribution of mPGES-1 expressed in either cell population to tumor progression has not yet been fully elucidated.

Although the inhibition of COX-2-mediated PGE_2 formation represents a promising chemopreventive strategy for reducing the risk of cancer, the cardiovascular side effects associated with COX-2 inhibitors, which most likely result from the blunting of anti-thrombotic prostacyclin (PGI_2), have recently been found to limit their use [22, 23]. From this viewpoint, selective blockage of the biosynthesis of PGE_2 without

affecting other prostanoids appears to be feasible for cancer chemoprevention with the potential for improved tolerability over NSAIDs. To better evaluate the efficacy of mPGES-1 inhibition in relieving symptoms of cancer, we herein used lung carcinoma cells with mPGES-1 knockdown (KD) or overexpression as well as mice null for mPGES-1. Our results provide evidence that mPGES-1 in both cancer cells and hosts contributes to tumorigenesis *in vitro* and *in vivo*.

EXPERIMENTAL

Cells

Lewis lung carcinoma (LLC) cells, which were originally isolated from the C57BL/6 mice, were cultured in Dulbecco's modified Eagle's medium (DMEM) containing 10% (v/v) fetal calf serum (FCS) under a humidified atmosphere containing 5% CO_2. To establish mPGES-1 KD and overexpressing LLC cells, we transfected these cells with a pRNA-U6.1/Hygro siRNA expression vector (GenScript, Piscataway, NJ) harboring an mPGES-1-directed siRNA target sequence (5'-GGCCTTTGCCAACCCCGAG-3' (residues 126-144 in the open reading frame) and a pcDNA3.1 expression vector (Invitrogen, Carlsbad, CA) containing mouse mPGES-1 cDNA, respectively, using lipofectamine 2000 (Invitrogen). After the transfection of these plasmids, LLC cells were cultured in medium containing 1 mg/ml G418 (Invitrogen) to establish stable clones. As a control, LLC cells transfected with an empty vector (pRNA-U6.1/Hygro or pcDNA3.1) were used (referred to as mock cells hereafter).

Animals

C57BL/6 and BALB/c mice were obtained from the Saitama Animal Center. mPGES-1 KO mice were established as described previously [12, 13], and backcrossed at least three generations with C57BL/6 mice or ten generations with BALB/c mice. Female mPGES-1 KO mice and littermate wild-type (WT) mice (7 weeks old) were used in each experiment. The mice were housed in microisolator cages in a pathogen-free barrier facility, and all experiments were conducted under approved institutional guidance.

Cell growth assay

Cells were seeded at 6 x 10^4 cells/well in 6-well plates or 1.5 x 10^5 cells/flask in T-25 culture flasks in culture medium in the presence or absence of 10 nM NS-398 (Cayman Chemicals, Ann Arbor, MI), a COX-2 selective inhibitor, or 1 mM 16,16-dimethyl PGE_2 ($dmPGE_2$) (Cayman Chemicals), a metabolically stable analog of PGE_2. After culture of 72 h, the cells were collected by trypsinization and counted in a Bright-line hemocytometer in the presence of trypan blue.

Western blotting

Aliquots of samples (20-μg protein equivalents) were subjected to sodium dodecyl sulfate-polyacrylamide gel electrophoresis (SDS–PAGE) using 10% (w/v) gels under reducing conditions. The separated proteins were electroblotted onto nitrocellulose membranes (Schleicher & Schuell, Hahnestr, Germany) with a semidry blotter (Bio-Rad, Hercules, CA). After blocking with 3% (w/v) skim milk in TBS (pH 7.4) containing 0.05% (v/v) Tween 20 (TBS–Tween), the membranes were probed with the respective antibodies for 2 h (1:2000 dilution for antibodies against mPGES-1 [14], mPGES-2 (Cayman Chemicals), cPGES (11), COX-1 and –2 (Santa Cruz Biotechnology, Santa Cruz, CA), EP1, 2, 3 and 4 (Cayman Chemicals), and vascular endothelial growth factor (VEGF) (Sigma, St. Louis, MO); and 1:2500 dilution for anti-mouse α–tubulin antibody (Zymed Laboratories, South San Francisco, CA) in TBS-Tween). After washing with TBS-Tween, the membranes were incubated with horseradish peroxidase-conjugated anti-goat (for COX-1, COX-2 and VEGF), anti-rabbit (for mPGES-1, mPGES-2,

cPGES, and EP1-4) and anti-mouse (for α-tubulin) IgG antibodies (1:5000 dilution in TBS–Tween) for 1 h, and visualized with the ECL Western blot system (Perkin Elmer Life Sciences, Boston, MA), as described previously [7, 13, 14].

Determination of PG levels

For the measurement of PGs in tissues, mouse tissues were washed twice with Hanks' solution containing 10 μM indomethacin (Sigma) before homogenization. The supernatants obtained from the tissue homogenates were adjusted to pH 3.0 with 1 N HCl and passed through a Sep-Pak C18 cartridge (Waters, Milford, MA), and the retained PGs were eluted with 8 ml of methanol, as described previously [13]. A trace amount of [^{3}H]PGE_2 (Cayman Chemicals) was added to the samples before passage through the cartridges to calibrate the recovery of the PGs. The sample solvents were evaporated, and then the PGs were dissolved in an aliquot of buffer and assayed with commercial enzyme immunoassay kits for individual PGs (Cayman Chemicals). Likewise, aliquots of the supernatants of cultured cells were subjected to the enzyme immunoassay for PGs.

Adhesion assay

Cells were plated at 2 x 10^5 cells in 35 mm dishes, which were pretreated with collagen, fibronectin or laminin (BD Biosciences, Billerica, MA). After incubation for 60 min at 37°C, the cells were fixed with Carnoy solution and then stained with Giemsa solution for 60 min. Adherent cells were counted in three fields at 40 x magnification using a microscope and J image software.

Invasion assay

Cell invasiveness was evaluated using a BD BioCoat™ Matrigel™ Invasion Chamber (BD Biosciences) according to the manufacturer's instructions. In brief, cells (1.2 x10^6 cells in 0.5 ml) suspended in DMEM containing 3% (v/v) FCS and 1% (v/v) sodium pyruvate (Invitrogen) were seeded on the top of the gel in each chamber. DMEM containing 10% FCS (0.75 ml) was added as a source of chemoattractants into the bottom wells of the plate. After 16 h of incubation, cells that had invaded onto the lower surface of the chamber were fixed with methanol for 5 min, and stained with crystal violet. Non-invasive cells on the upper surface were removed with a cotton bud, and the membrane was cut. The number of invading cells was quantified by counting them under a light microscope. Statistical significance was determined by the Student's *t*-test.

Tumor implantation model

One million LLC cells in 100 μl of phosphate-buffered saline (PBS) were injected subcutaneously into 8-wk-old female mice. Tumor growth was assessed by the measurement of two bisecting diameters in each tumor using calipers. The size of the tumor was determined by direct measurement of the tumor dimensions. The volume was calculated according to the equation ($V = (L \times W^2) \times 0.5$), where V = volume, L = length, and W = width (36). On day 14 after tumor implantation, the mice were anesthetized and killed by dislocation of the cervical spine, and the tumor tissues were dissected, weighed, and then fixed in 10% (v/v) formalin for histochemical analyses. The intratumoral blood vessels in the most intensive neovascularization areas were quantified by staining of the sections with hematoxylin and eosin followed by silver. For each tumor, five random images were captured at x400 magnification. Only areas of viable tumor tissue were imaged; necrotic regions were excluded. The individual microvessels were counted. The structure of individual microvessels was clearly differentiated from tumor cells on silver staining. The final vascular density score for the tumor represents an average of all scored fields.

Lung metastasis model

One million LLC cells in 100 μl of PBS were intravenously injected in the lateral tail veins of 8-wk-old female mice. Then, 14 days later, the mice were anesthetized and killed, and the lungs were removed and weighed. Finally, the lungs were placed in Bouin's solution for 24 h and then photographed.

Determination of hemoglobin levels in tumor tissues

The dissected tumor tissues were washed, cut into small pieces with scissors, and homogenized with a Polytron homogenizer in a SET buffer (250 mM sucrose, 0.5 mM EDTA, and 20 mM Tris–HCl (pH 7.4)) containing 10 mM indomethacin, 1 mM phenylmethylsulfonyl fluoride, and 0.5% (v/v) Triton X-100. The tissue homogenates obtained were centrifuged at 3,000 rpm for 5 min, and an aliquot (200 μl) of the supernatant was centrifuged again at 14,000 x g for 30 min at 4°C. Concentrations of hemoglobin in the supernatant were then determined spectrophotometrically by measuring the absorbance at 540 nm using a hemoglobin assay kit (Wako, Osaka, Japan).

RT–PCR

Total RNA was isolated from cells and tissues using Trizol (Invitrogen). Synthesis of cDNA was performed with 2 μg of the total RNA and avian myeloblastosis virus-reverse transcriptase according to the manufacturer's instructions supplied with the RNA PCR kit version 2.1 (Takara Biomedicals, Shiga, Japan). Subsequent amplifications of the partial cDNA fragments were performed using 0.5 μl of the reverse-transcribed mixture as a template with a set of specific oligonucleotide primers (Sigma) as follows: mouse VEGF, sense 5'-GATGAAGCCCTGGAGTGC-3' and antisense 5'-TCCCAGAAACAACCCTAA-3'; and mouse glyceraldehyde-3-phosphate dehydrogenase (GAPDH), sense 5'-TCGTGGATCTGACGTGCCGCCTG-3' and antisense 5'-CACCACCCTBTTGCTGTAGCCGTAT-3'. The PCR mixtures were subjected to 30 cycles of amplification by denaturation (30 s at 94°C), annealing (30 s at 57°C), and elongation (30 s at 72°C). The PCR products were analyzed by 1% agarose gel electrophoresis with ethidium bromide.

Real-time RT-PCR

Single-stranded cDNA was generated using 1 μg of total RNA as a template and avian myeloblastosis virus reverse transcriptase, using a High Capacity Reverse Transcriptase kit (Applied Biosystems, Foster City, CA). Real-time PCR was carried out using the SYBR Green PCR Master Mix (Applied Biosystems) and StepOne (Applied Biosystems) according to the manufacturers' instructions. The PCR primer sets used were 5'-ATGGCTCAGACATCCACTCC-3' and 5'-GGTCATCTAGCCCATCTCCA-3' for mouse α5 integrin and 5'-GGTGTCGTGTTTGTGAATGC-3' and 5'-TGACGCTAGACATGGACCAG-3' for mouse β1 integrin. The expression levels of the integrins were normalized with those of mouse GAPDH with a primer set of 5'-ATGTGTCCGTCGTGGATCTGA-3' and 5'-ATGCCTGCTTCACCACCTTCT-3'. Results represent an average of three independent experiments.

Gelatin zymography

Lysates of cells and tissues (27-μg protein equivalents) were subjected to 10% SDS–PAGE, with 1 mg/ml gelatin substrate being incorporated into the gels. Following electrophoresis, the gels were soaked in 2.5% Triton X-100 to remove SDS, rinsed with 10 mM Tris–HCl, pH 8.0, and transferred to a bath containing 50 mM Tris, pH 8.0, 5 mM $CaCl_2$, and 1 μM $ZnCl_2$ at 37°C for 18 h. The gels were then stained with 0.1% Coomassie blue in 45% methanol and 10% acetic acid.

RESULTS

Reduced tumorigenic potential of mPGES-1-silenced LLC cells in vitro — We established mPGES-1

KD LLC cells by means of an siRNA silencing strategy, as described in Experimental Procedures. The expression levels of mPGES-1 and other enzymes involved in PGE_2 synthesis in mPGES-1 KD and mock cells were examined by Western blotting (Fig. 1A). The expression level of mPGES-1 was reduced by ~80% in mPGES-1 KD cells relative to mock cells, while those of COX-1 and -2 and other PGE synthases (cPGES and mPGES-2) in both cell lines were approximately the same (Fig. 1A). Furthermore, we found that, among the four EP receptor subtypes that can bind to PGE_2 [24], LLC cells expressed detectable levels of EP2, EP3 and EP4 proteins, among which the level of EP2 protein was slightly reduced in mPGES-1 KD cells relative to mock cells (Fig. 1A). The amounts of PGE_2 released into medium during culture were decreased in mPGES-1 KD cells relative to mock cells (Fig. 1B), whereas those of 6-keto $PGF_{1\alpha}$ (a non-enzymatic hydrolytic product of PGI_2) and $PGF_{2\alpha}$ were comparable between mPGES-1 KD cells and mock cells (Fig. 1C).

Concurrently, mPGES-1 KD cells grew more slowly than did mock cells (Fig. 1D). NS-398, a COX-2-selective inhibitor, suppressed PGE_2 generation and cell proliferation in mock cells by ~60% and ~25%, respectively, whereas no further decreases in PGE_2 production and cell growth were found in mPGES-1 KD cells (Fig. 1B and D). Production of 6-keto $PGF_{1\alpha}$ and $PGF_{2\alpha}$ was equally sensitive to NS-398 in both cell lines (Fig. 1C). Furthermore, cell growth of mPGES-1 KD cells was partially (even if not completely) restored by addition of an optimal concentration (1 μM) of 16,16-dimethyl PGE_2 ($dmPGE_2$), a synthetic analog of PGE_2 (Fig. 1E). These results suggest that the PGE_2 produced through the COX-2/mPGES-1 pathway is partially required for the proliferation of LLC cells.

In the process of tumor metastasis, cancer cells from the primary tumor must invade the extracellular matrix (ECM). There are many reports demonstrating that malignant tumor cells often possess high invasive activity [25]. Thus, we next assessed the effect of mPGES-1 silencing on the invasive activity of LLC cells using Matrigel™ invasion chambers. As shown in Fig. 2A, the number of mPGES-1 KD cells migrating across the Matrigel-coated filter was markedly fewer than that of mock cells. Since it is known that the PGE_2 signaling activates the invasive potential of cancer cells by increasing the expressions of VEGF, a proangiogenic factor, and matrix metalloproteinases (MMPs), which hydrolyze type IV collagen localized in the basement membrane [25], we next examined the effects of mPGES-1 silencing on the expression of VEGF and the activities of MMP-2 and -9 by Western blotting and gelatin zymography, respectively. As shown in Fig. 2B, MMP-2 activity in the conditioned medium from mPGES-1 KD cells was lower than that in the medium from mock cells. In contrast, MMP-9 activity and VEGF expression were unaffected by mPGES-1 silencing (Fig. 2B). These results suggest that the silencing of mPGES-1 diminishes *in vitro* migration of LLC cells by reducing the PGE_2-induced MMP-2 activation.

The ability of cancer cells to adhere to the ECM influences their motility and invasion in tumor tissues *in vivo*, and metastatic tumor cells show decreased ECM-adherent activity *in vitro* [25, 26]. Therefore, we next studied the attachment of mPGES-1 KD or mock cells to culture dishes pre-coated with distinct ECM components. The results showed that the numbers of mPGES-1 KD cells adhering to collagen and fibronectin, but not to laminin, were significantly increased as compared with those of mock cells (Fig. 2C). Moreover, the increased adhesion of mPGES-1 KD cells to collagen or fibronectin was entirely reversed by $dmPGE_2$ to the level of mock cells (Fig. 2C). Consistent with the increased binding of mPGES-1 KD cells to collagen and fibronectin, the expressions of their receptor components, α5 and β1 integrins, were elevated in the KD cells relative to control cells (Fig. 2D). Thus, we conclude that mPGES-1 supplies a majority of the PGE_2 that enhances the malignant potential (in terms of ECM invasion and adherence) of